THE HONG KONG INSTITUTION OF ENGINEERS 香港工程師學會

Long-term performance of hybrid MiC buildings considering concrete creep and shrinkage

Yingqi Liu[1,2], Ho Kit Siu[2,3], Shiyu Guan[4], and Francis T K Au[2]

[1] School of Transportation and Logistics Engineering, Wuhan University of Technology, Wuhan, Hubei Province, People's Republic of China

[2] Department of Civil Engineering, The University of Hong Kong, Hong Kong, People's Republic of China

[3] Water Supplies Department, The SAR Government, Hong Kong, People's Republic of China

[4] China Construction Third Bureau First Engineering Co., Ltd. Wuhan, Hubei Province, People's Republic of China

ABSTRACT

With the completion of several pilot projects in Hong Kong, Modular Integrated Construction (MiC) is being promoted to boost the productivity and cope with the labour shortage in the local construction industry. However, the possible adverse effects of differential axial shortening due to the time-dependent behaviour arising from concrete creep and shrinkage will only become obvious after a long time. In this study, simplified numerical models are established based on typical hybrid MiC buildings in Hong Kong. Time-dependent analyses considering the creep and shrinkage of concrete are carried out. The construction schedules of the pilot MiC projects are used as a reference to model the staged construction. The results for a 20-storey hybrid MiC building indicate, owing to the concrete creep and shrinkage, noticeable stresses at the module-to-wall connections at the corners of core walls 30 years after construction. The compressive stresses at the bottom of the steel MiC modules will increase substantially over time, which could reduce the amount of material strength that can be utilised by other loads. Hence checking of long-term performance should be conducted at the design stage, particularly focusing on the connections.

KEYWORDS Bolted connection; creep and shrinkage; hybrid MiC building; long-term performance; numerical modelling; staged construction analysis

CONTACT Francis T K Au francis.au@hku.hk

Received 24 October 2022

1. Introduction

Modular-integrated Construction (MiC) has recently become a hot topic in the construction industry. It can be adopted in the construction of residential buildings and hotels. Normally, the modular units with completed finishes and fixtures are prefabricated in factories and transported to site for assembly afterwards. The MiC structure is then built by stacking the modules together with the connections carried out on site. Compared to the traditional construction method that relies heavily on the labour-intensive work on site, adoption of MiC can bring various advantages including enhanced quality control, shorter construction time, improved site safety as well as reduced construction waste (Wang and Pan, 2020; Wang et al., 2020). The construction industry in Hong Kong has encountered a critical shortage of workforce due to the ageing workforce and insufficient manpower replenishment. With the dwindling workforce, it is not surprising that the construction cost in Hong Kong has been ranked the second most expensive worldwide (Pan and Hon, 2018). In this regard, MiC can be a way forward to meet the development needs in the future. MiC was mentioned in the Policy Address 2017 of the HKSAR Government as an innovative approach in the construction industry (Pan and Hon, 2018). Over the past few years, several pilot projects have been launched such as the 17-storey InnoCell in Hong Kong Science Park (Figure 1), the 16-storey discipline services quarters for the Fire Services Department at Tseung Kwan O, and the Quarantine Camp in Penny's Bay (Construction Industry Council, no date).

Despite the benefits mentioned above, the application of MiC to truly high-rise buildings is rare. The tallest building constructed by MiC in the world is the 44-storey residential building at 101 George Street, Croydon, London (Construction Industry Council, no date). One of the tallest MiC buildings under construction in Hong Kong is the 23-storey private residential tower at Tai Kok Tsui (Construction Industry Council, no date). Compared to low- to medium-rise structures, high-rise buildings are often governed by the design wind or seismic loading. A widely adopted solution is to cast the reinforced concrete (RC) core walls in situ to ensure a certain amount of lateral resistance before the erection of prefabricated steel-frame modules connected by means of bolting (Wang and Pan, 2020), producing a steel-concrete hybrid MiC building.

The core walls in high-rise hybrid MiC buildings often provide the required lateral resistance under extreme wind or seismic loading conditions. However, high-rise buildings may also suffer from possible adverse effects of the time-dependent behaviour of concrete. In the typical design of RC buildings, the creep and shrinkage strains of different concrete members vary over time, causing additional internal forces and stress redistribution in the whole structure (Blanc et al., 2021). Attention was firstly drawn to this problem in the 1960s, where excessive deflection and even cracking in slabs and beams were observed in buildings with over 30 storeys (Moragaspitiya et al., 2010; Zou et al., 2019). In the context of high-rise hybrid MiC buildings, the combined use of steel modules and RC core walls exhibits differential axial shortening in the vertical compression members. Steel at relatively low sustained stress levels, i.e. below 55% yield stress, does not exhibit time-dependent behaviour (Au and Si, 2011), while the creep of concrete is often assumed to be proportional to the concrete stress in the range of working stress. It is therefore expected that only the cast in situ RC core walls undergo secondary axial shortening over time whilst the time-dependent deformation of typical steel columns under sustained stress of low level is negligible. The resulting differential axial shortening is envisaged to be more significant compared to that in ordinary buildings built entirely of RC. On the other hand, the casting of RC core walls and the subsequent work on the inter-module and module-to-core connections is carried out floor by floor from the base. The compressive load borne by the lower vertical members increases with the construction of each subsequent floor. The load-time history analysis is crucial to the evaluation because the concrete age at loading and the duration of loading are the key factors affecting the development of creep and shrinkage (Zou et al., 2014).

Figure 1. The 17-storey InnoCell in Hong Kong Science Park.

Therefore, the possible adverse effects due to the time-dependent behaviour arising from concrete creep and shrinkage might be a concern for hybrid MiC buildings adopting steel-framed modules and RC core walls. In this study, the long-term performance of a typical 20-storey hybrid high-rise MiC building considering the creep and shrinkage behaviour of concrete is evaluated by numerical simulation using the structural package SAP2000 (CSI, 2000). Recommendations from the CEB-FIP Model Code 2010 (fib, 2010) are used to describe the time-dependent behaviour of concrete for convenience, and the construction schedules of pilot MiC projects are used as a reference to model the staged construction. The long-term axial shortening in the RC core walls due to creep and shrinkage, and the internal forces induced in various structural members are analysed. With all the results obtained, it is suggested that checking of the long-term performance should be conducted at the design stage for hybrid MiC buildings with RC core walls and steel-framed modules.

2. Elastic, creep and shrinkage strains in concrete

In the behaviour of concrete material, creep represents the deformation due to the breakage and reformation of atomic bonds in areas under significant stress within the colloidal microstructure of the calcium silicate hydrate gels in the hardened cement paste (Bažant and Jirásek, 2018). It is directly related to the stress applied to the concrete member. Unlike creep, shrinkage is independent of the compressive stress experienced by concrete. In a dry environment, concrete shrinks slowly due to the evaporation at the concrete surface resulting in the diffusion of water particles out of the cement gel pores (Bažant and Jirásek, 2018). Under constant relative humidity, the observed shrinkage strain gradually increases over time, but at a decreasing rate.

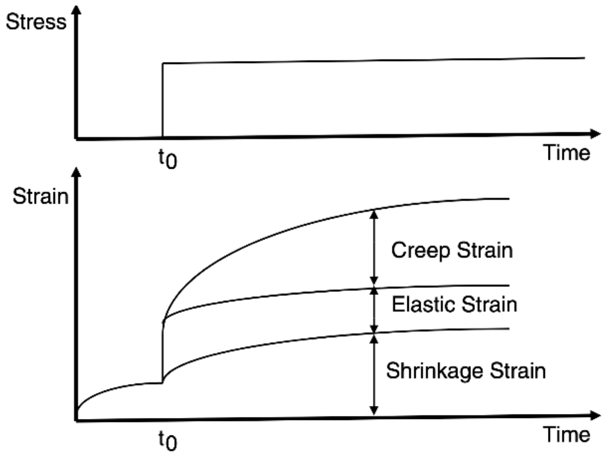

Figure 2. Stress-strain relationship of concrete under an applied load.

Neglecting the self-weight of the concrete member, shrinkage begins once the concrete member is cast and particularly when curing ceases. When a load is applied to the member, an instant elastic strain is produced. Under constant loading, the elastic strain remains unchanged whilst the creep strain develops over time. Therefore, the total strain of the concrete member after time t_0 consists of these three components as shown in Figure 2. Researchers have previously developed multiple models to evaluate the creep and shrinkage behaviour of concrete material, such as CEB-FIP Model Code 2010 (fib, 2010), ACI 209R-92, and Bažant-Baweja B3 (Bažant and Jirásek, 2018). The formula in Eurocode 2 (Blanc et al., 2021; British Standards Institution, 2005), is adopted, i.e.

$$\varepsilon_c(t) = \varepsilon_{ci}(t_0) + \varepsilon_{cc}(t) + \varepsilon_{cs}(t)\,, \qquad (1)$$

where $\varepsilon_{ci}(t_0)$ is the instantaneous elastic strain due to the concrete stress $\sigma_c(t_0)$, $\varepsilon_{cc}(t)$ is the creep strain and $\varepsilon_{cs}(t)$ denotes the shrinkage strain.

2.1. Instantaneous elastic strain $\varepsilon_{ci}(t_0)$

When a compressive load is applied to a concrete member at time t_0, the instantaneous elastic strain $\varepsilon_{ci}(t_0)$ induced can be described as $\varepsilon_{ci}(t_0) = \sigma_c(t_0)/E_{ci}(t_0)$, where $E_{ci}(t_0)$ is the modulus of elasticity of concrete at time t_0. Owing to the continuous cement hydration in the hardened concrete, the concrete gradually becomes stiffer, and its elastic modulus increases over time at a decreasing rate, as shown plotted against the logarithmic scale of time in Figure 3.

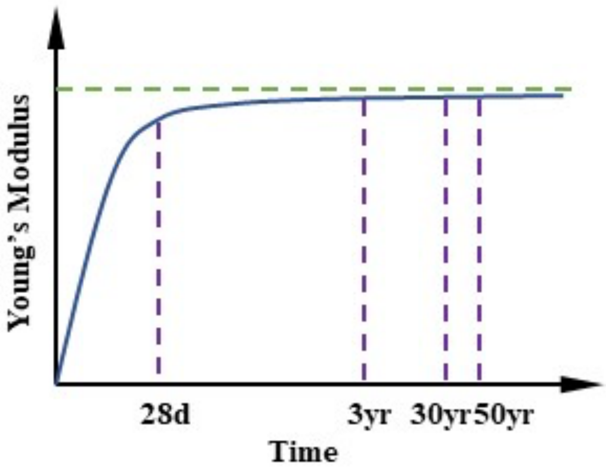

Figure 3. Development of modulus of elasticity of concrete over time.

The time-dependent modulus of elasticity $E_{ci}(t)$ of concrete can be estimated by $E_{ci}(t) = \beta_E(t)E_{ci}$, where E_{ci} is the elastic modulus of concrete at 28 days and the coefficient $\beta_E(t)$ is dependent on the age of concrete t (days) only. The instantaneous elastic modulus of concrete is critical for obtaining accurate results in the subsequent time-dependent analysis, which describes the varying material property of concrete during the construction of the whole building. Neglecting the instantaneous concrete elastic modulus or disabling the stepped construction function during building erection would lead to inaccurate simulation results. The detailed construction sequence of the hybrid MiC building will be discussed later in Section 3.

2.2. Creep strain $\varepsilon_{cc}(t)$ and shrinkage strain $\varepsilon_{cs}(t)$

The creep strain $\varepsilon_{cc}(t)$ and shrinkage strain $\varepsilon_{cs}(t)$ are also governed by their respective coefficients. Particularly, for a constant stress applied at time t_0, the creep strain is evaluated as $\varepsilon_{cc}(t,t_0) = [\sigma_c(t_0)/E_{ci}\phi]\cdot\phi(t,t_0)$, where $\phi(t,t_0)$ is the creep coefficient given by

$$\phi(t,t_0) = \phi_{bas}(t,t_o) + \phi_{dry}(t,t_o)\,, \qquad (2)$$

where $\phi_{bas}(t,t_o)$ is the basic creep coefficient and $\phi_{dry}(t,t_o)$ is a drying creep coefficient. Considering the creep development at time t after constant loading since time t_0, both of the above-mentioned creep coefficients are associated with the mean 28-day compressive strength of concrete f_{cm}. The drying creep coefficient is also dependent on the relative humidity RH (%) of the environment and the notional size of member h (mm).

Similarly, the concrete strain due to shrinkage can be estimated by

$$\varepsilon_{cs}(t,t_s) = \varepsilon_{auto}(t) + \varepsilon_{dry}(t,t_s)\,, \qquad (3)$$

where ε_{auto} is the autogenous shrinkage and $\varepsilon_{dry}(t,t_s)$ is the drying shrinkage. Autogenous shrinkage ε_{auto} is dependent on the shrinkage development at time t, the mean 28-day compressive strength of concrete f_{cm}, and the type of concrete. The drying shrinkage $\varepsilon_{dry}(t,t_s)$ is also dependent on the relative humidity RH (%), the notional size of member h (mm) and the age of concrete (days) when shrinkage begins t_s.

To sum up, except for the time variables such as age t, t_0 and t_s, the above formulae in the CEB-FIP Model Code 2010 (fib, 2010) indicate that four additional parameters should be provided for time-dependent analysis of concrete structures, including the type of cement, notional size of member h, relative humidity RH, and compressive strength of concrete f_{cm}.

3. Establishment of the hybrid MiC structural model in SAP2000

The structural model was constructed using the built-in time-dependent material behaviour feature and the stepped construction function in the computer package

SAP2000. The modelling of creep and shrinkage behaviour of concrete members based on CEB-FIP Model Code 2010 (fib, 2010) could be conducted without the need for manual adjustment of the elastic modulus for different load stages.

3.1. Configuration of the hybrid MiC building

Since the design of structural elements of the MiC building is not the main focus of this paper, the hybrid building studied by Shan et al. (2019) and Shan and Pan (2020) was taken as a reference for the subsequent modelling work, which was based on Shun Hing College of Jockey Club Student Village III of The University of Hong Kong. This is a 31-storey building constructed by the traditional cast-in-situ approach. Figure 4 shows the building plan of about 24 m × 15.2 m with a gross floor area of 315 m^2.

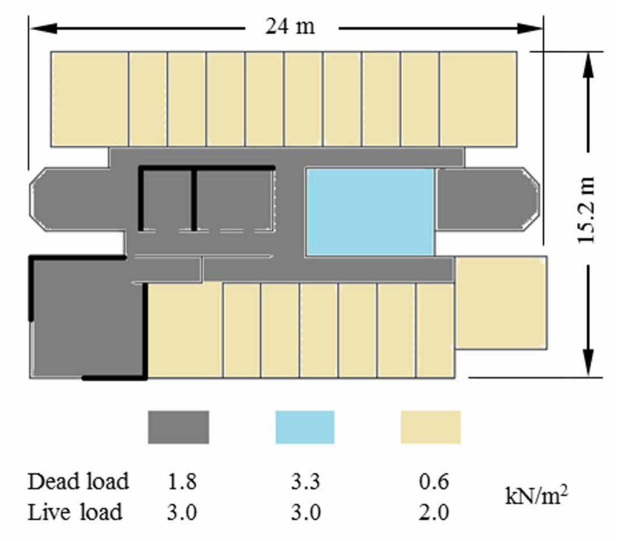

Figure 4. Floor plan of Shun Hing College.

The three-dimensional (3D) view of the proposed 20-storey hybrid MiC building model adopted in this study is shown in Figure 5. In this structural model, the red, deep blue and light blue lines represent the steel beams, columns and bracings of the modules, respectively. The RC core walls and RC floor slabs are shown as green and grey areas, respectively. Instead of the 31 storeys in accordance with the reference student residence building, the simplified structural model studied was trimmed down to 20 storeys since it would be close to the existing tallest MiC high-rise buildings in Hong Kong. The storey height was taken as 3 m, giving the overall building height of 60 m. Figure 6 shows the simplified floor plan of the 20-storey model for analysis, with the connections between the core wall and the steel modules indicated, while the module-to-core wall connections along the white gaps are omitted for clarity. Each of the longer sides of the 6 m wide RC core walls is connected to 12 steel modules with dimensions of 4 m (L) × 2 m (W) × 3 m (H). Minor adjustment was applied to the module dimensions to facilitate convenient modelling. Moreover, the concrete core was also slightly revised to have a more regular arrangement for simpler interpretation of the results. The revised core arrangement allowed for the space required for installation of lifts (8 m (L) × 3 m (W)) and staircases (2 m (L) × 3 m (W)). The nodes at the lowest floor of the building were set to be pinned to a solid foundation.

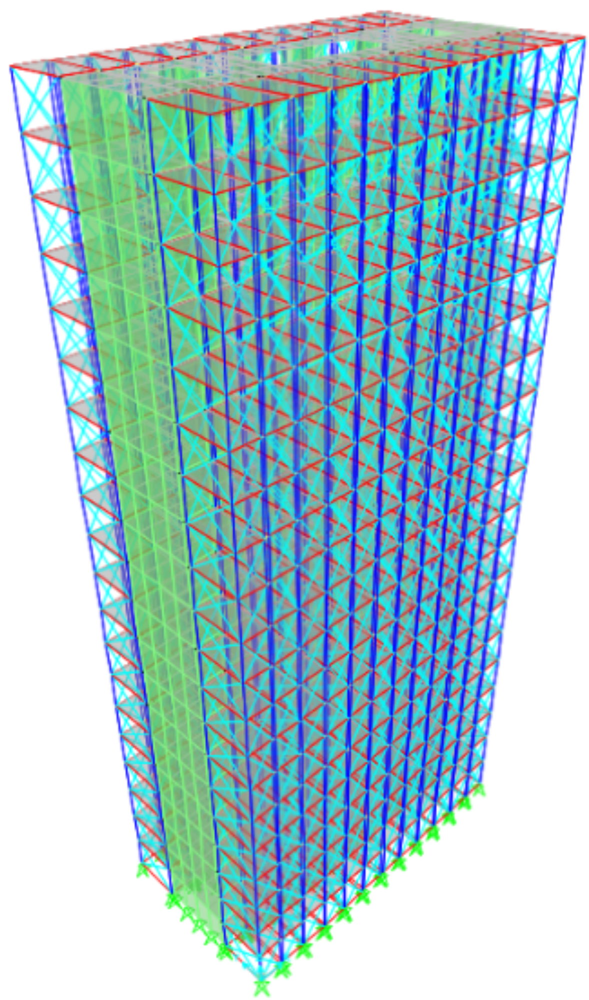

Figure 5. 3D view of the hybrid MiC building model.

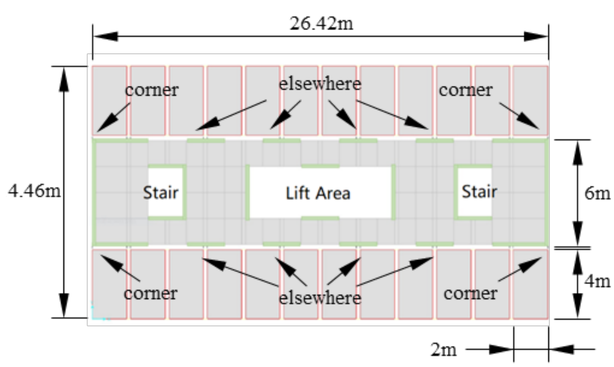

Figure 6. Floor plan of the hybrid MiC building model.

3.2. Material properties

Three different building materials were used in developing the hybrid MiC model. Grade S355 medium tensile steel was used for the frame members in the steel modules, Grade S690 high-strength steel was adopted for the anchor rods in connections, and Grade 45 concrete was assumed for the RC core walls and RC slabs, largely according to the structural model of Shan and Pan (2020). The default material properties of the corresponding concrete and steel materials were used in SAP2000. For the RC core walls, the time-dependent properties of concrete were adopted based on CEB-FIP Model Code 2010 (fib, 2010), including (a) the increase of compressive strength and stiffness over time, (b) the creep effect, and (c) the shrinkage effect. Historical data from the Hong Kong Observatory show that the monthly mean of relative humidity (RH) in Hong Kong ranges from 70% to 83% (Hong Kong Observatory, 2022). Thus, an RH value of 75% was used in the model to reflect the ambient conditions of the MiC building in Hong Kong. The core walls were constructed on site with 7-day curing, after which shrinkage begins. Default values for the creep and shrinkage parameters were adopted for the RC core walls as summarised in Table 1. The ultimate shrinkage strain was estimated to be 296×10-6 according to the code (fib, 2010). To ensure the computational efficiency, only the time-dependent material properties of the RC core walls were considered in the time-dependent analysis, but those of the concrete slabs were ignored.

Table 1. Creep and shrinkage parameters for the RC core walls.

Parameter	Value
Cement type	**42.5 N**
Relative humidity (RH)	**75%**
Age when shrinkage begins (t_s)	**7 days**
Cylinder compressive strength of concrete (f_{cm})	**45 MPa**

3.3. Sectional properties of different members

The frame structure of the single steel module as shown in Figure 7 is normally formed by Grade S355 rectangular hollow sections (RHS) without load-bearing module walls. The sectional properties adopted by Shan and Pan (2020) were used for developing the model, i.e. RHS 200 mm × 200 mm × 12.5 mm (thickness) for the columns, RHS 200 mm × 150 mm × 12.5 mm for the beams and RHS 100 mm × 100 mm × 6 mm for the bracing members. It is assumed that the steel members of each module are rigidly connected at the joints by welding during their off-site prefabrication.

For the concrete members, shell elements with thicknesses of 400 mm and 150 mm were adopted for the Grade 45 RC core walls and RC slabs of the simplified building model, respectively. However, the time-dependent material properties of concrete were only considered for the core walls as mentioned in Section 3.2.

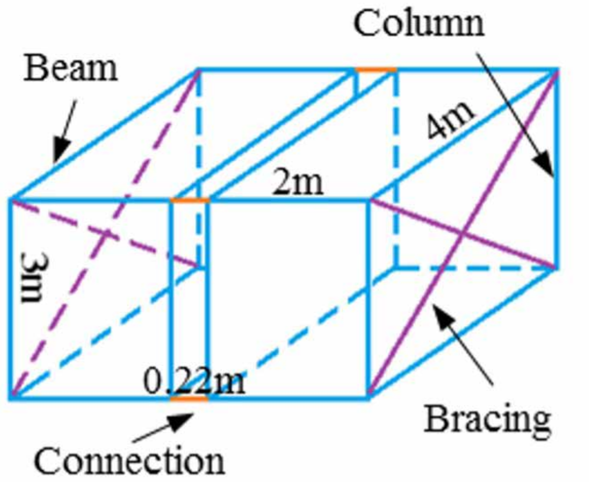

Figure 7. Frame structure of a single module (based on (Shan et al., 2019)).

For the connections shown in orange, the inter-module connection and module-to-core connection adopted by Shan and Pan (2020) were applied to the present structural model. Firstly, a 150 mm width × 12 mm thick tie plate of Grade S355 steel was used as the horizontal connection between adjacent modules on the same floor. The length of the tie plate was 220 mm including a 20 mm construction tolerance. Both ends of the tie plate were pinned such that no moment transfer would take place between the modules. Secondly, the vertical connection between two modules of consecutive floors was simplified as pinned because the number of anchor rods used there were too few to be regarded as a moment connection.

The module-to-core connections of Shan and Pan (2020) were adopted in the present model, comprising two 39 mm diameter Grade S690 steel anchor rods with a length of 320 mm placed at 280 mm vertical intervals as shown in yellow in Figure 8(a). A user-defined cross section was adopted for the module-to-core frame element in the structural model, considering the actual layout of anchor rods. The total length of the module-to-core frame element (Figure 8) was 320 mm including a 200 mm rigid segment and a 120 mm pinned segment. The short segment shown in green in Figure 8(b) was pinned to the longer segment shown in orange to simulate a bolted connection. The longer segment was fixed to the RC core wall shell elements and a high stiffness modifier of 100 was applied to the longer segment to simulate a 200 mm rigid arm embedded in the RC core walls.

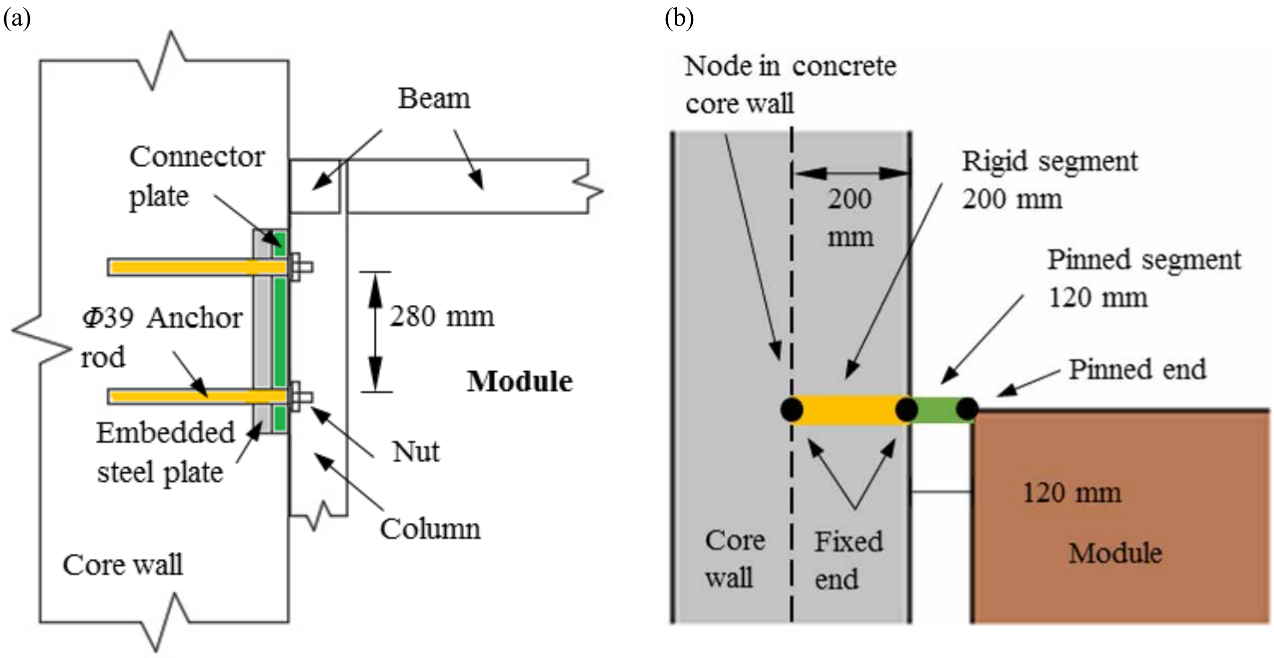

Figure 8. Module-to-core bolted connections: (a) actual details; and (b) idealised model based on Bažant and Jirásek (2018) and British Standards Institution (2005).

Table 2. Details of defined stages for construction of the hybrid MiC building.

Stage No.	Duration (day)	Description	Cumulative days		Stage No.	Duration (day)	Description	Cumulative days
1	0	Construction began	0		20	20	19-20 CwS + 9-14 M	200
2	20	1-2 CwS	20		21	0	DL_19-20 CwS + 9-14 M	200
3	0	DL_1-2 CwS	20		22	20	15-20 M + DL_15-20 M	220
4	20	3-4 CwS	40		23	0	Construction completed	220
5	0	DL_3-4 CwS	40		24	60	SDL+0.25LL on floors	280
6	20	5-6 CwS	60		25	85	Year 1	365
…	…	…			26	365	Year 2	730
14	20	13-14 CwS	140		27	365	Year 3	1095
15	0	DL_13-14 CwS	140		28	365	Year 4	1460
16	20	15-16 CwS	160		29	365	Year 5	1825
17	0	DL_15-16 CwS	160		30	365	Year 10	3650
18	20	17-18 CwS + 1-8 M	180		31	365	Year 20	7300
19	0	DL_17-18 CwS + 1-8 M	180		32	365	Year 30	10950
	Legend: CwS – add Core wall and Slab elements; M – add Module elements; F – floor; DL – activate Dead Load; SDL – activate Superimposed Dead Load; LL – activate Live Load; 1-2 – floor No.							

3.4. Loading and staged construction

Since the emphasis of this paper is the long-term performance of buildings considering the creep and shrinkage behaviour of concrete, only the permanent vertical loads were considered in the structural model. The transient loads due to wind and seismic effects were neglected in the analysis. Dead loads were automatically calculated based on the self-weight of the members. The unit weights of concrete and steel were taken as 25 kN/m^3 and 77 kN/m^3, respectively. On every floor, the superimposed dead load was 2 kPa, covering the weight of the floor finishes and building services, while the imposed load was determined as 3 kPa in accordance with the Code of Practice for Dead and Imposed Load (Buildings Department, 2011). For evaluation of the long-term performance, only 25% of live load was assumed to account for its variation. The partial safety factor was taken to be 1.0 for all the permanent vertical loads for the investigation of long-term serviceability limit state performance.

The unique construction sequence of a typical hybrid MiC building is believed to have a significant impact on the development of creep and shrinkage strains in the structure. The erection of the hybrid MiC building was simulated by the Staged Construction load case in SAP2000. By defining various construction steps with certain durations in the stage tree, various members and the corresponding loads can be added or distributed in accordance with the construction sequence, while structural analysis can be conducted with results generated at the end of every defined step.

In most conventional building projects in Hong Kong, a 7-day cycle is usually adopted for the erection of each storey. For the local MiC building Innocell, a 4-day cycle was successfully implemented for installation of modules (WSP Co. Ltd., 2022). Therefore, to optimise the construction programme, the construction of the RC core walls started ahead of the MiC module installation. A 20-day cycle was arranged for casting every two storeys of the RC core walls and erecting every group of 6 to 8 storeys of steel-frame modules. In-situ construction of the RC core walls commenced on Day 0. Upon completion of the RC core walls at Storey 16 on Day 160, installation of the steel-frame modules first commenced in parallel with the casting of the remaining part of RC core walls after Storey 16. The entire building was completed on Day 220, while the Superimposed Dead Load and Live Load were applied after two months on Day 280. The construction stages for the hybrid MiC building are given in Table 2 and partly illustrated in Figure 9.

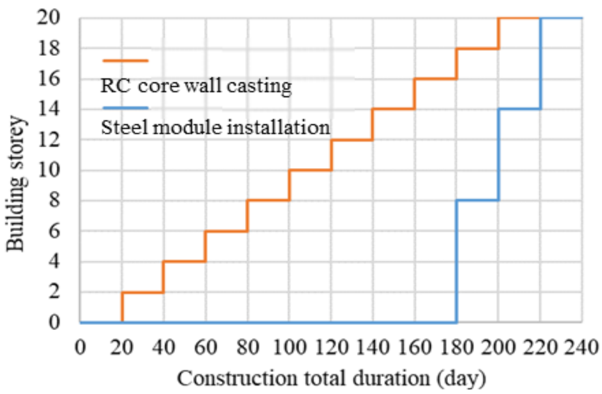

Figure 9. Programme of first 22 stages for construction of the hybrid MiC building.

4. Long-term performance

Results of the long-term deformation and changes in the internal stresses of various structural members at different stages were reviewed and analysed. In view of the symmetric arrangement of the hybrid MiC structural model, detailed results are presented for selected elements only.

The maximum downward displacement of the core wall at the top storey in Year 30 (Stage 32) is about 16.0 mm, which is far above the 5.0 mm in Year 1 and the 2.5 mm obtained by ignoring the time-dependent properties. Figure 10 shows the overall building deformations of the hybrid MiC model under the permanent vertical loads at Year 1 (Stage 25) and Year 30 (Stage 32). The RC core walls shown in green undergo vertical shortening over time. Since there is no change in applied loading after Stage 23, the axial shortening of the core walls is attributed to the combined effects of concrete creep and shrinkage behaviour.

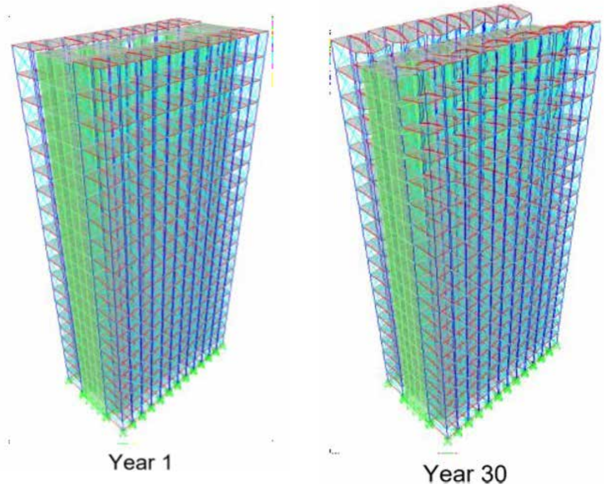

Figure 10. Overall deformation of the hybrid MiC structural model at Year 1 and Year 30 (scaled up 400 times).

(a)

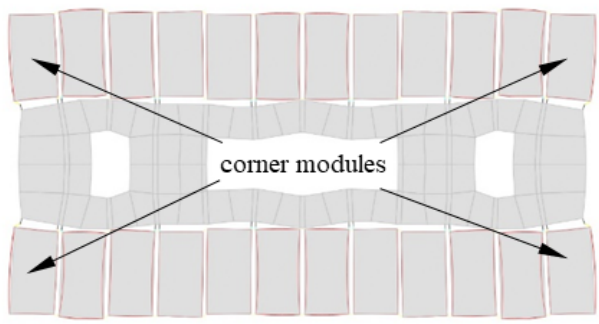

(b)

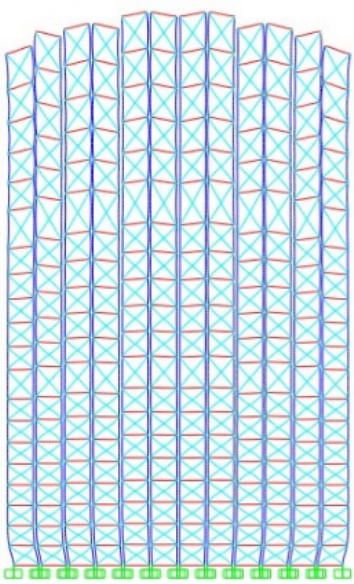

(c)

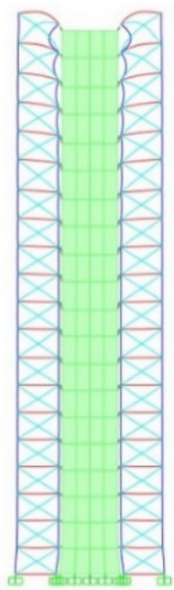

Figure 11. Deformation of the hybrid MiC structural model at Year 30: (a) plan; (b) front view; and (c) side view (scaled up 5,000 times).

4.1. Long-term deformation

Figure 11 with a higher scaling factor for overall deformation shows the 3D size reduction of the core walls. The core walls will experience not only vertical shortening, but also inward movements, which explains the flexural deformation of the steel members at the uppermost storey.

4.2. Long-term vertical stress of core walls

Since the core walls were modelled by shell elements, the shell component S22 provides the vertical stress carried by the core walls, with compressive stresses taken as negative. To investigate the long-term stress variations in the core walls, the stress distributions of the front and side panels at different stages are shown in Figure 12.

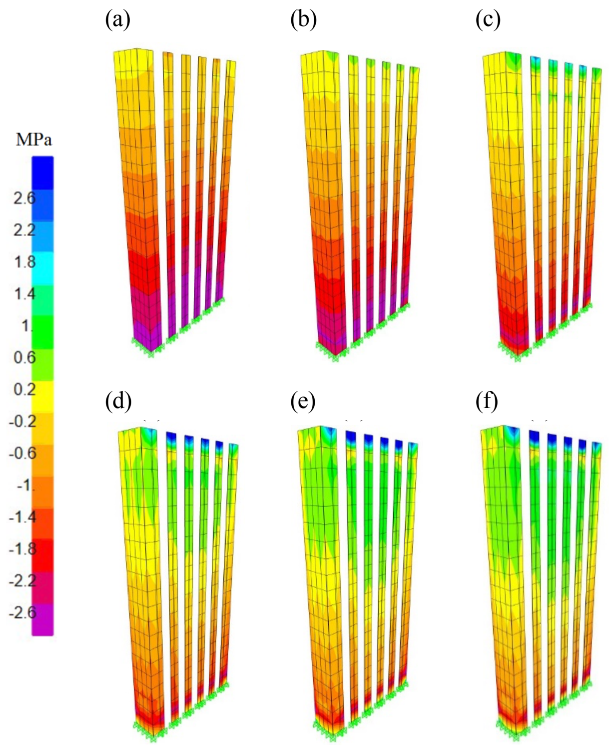

Figure 12. Vertical stresses in selected core walls: (a) ignoring time-dependent behaviour; (b) Year 1; (c) Year 3; (d) Year 10; (e) Year 20; and (f) Year 30.

With the continual development of concrete creep and shrinkage strains, the core walls tend to shorten further. Therefore, the vertical compressive stresses borne by the core walls reduce over time as some of the vertical gravity load gradually redistributes from the RC core walls to the steel columns that remain elastic. Ignoring concrete time-dependent behaviour, tensile stress is only observed as light-yellow zones at the top corners and the maximum compressive stress of 3.0 MPa occurs at the bottom storey of the core walls. When considering the time-dependent behaviour, tensile stresses show up at Year 1 already and increase quickly at the uppermost storey over time. Additional tensile stresses develop at the upper part of the building and propagate downward over time. Figure 12(f) shows a mixture of tensile and compressive stresses distributed at the bottom storey at Year 30. Obviously, noticeable shear and bending moments are induced at the base of core walls in the long run due to concrete creep and shrinkage. If this long-term behaviour of concrete is not considered, it may reduce the available amount of material strength that can be utilised by other loads, such as typhoon wind loads, acting on the hybrid MiC building in the future.

4.3. Long-term axial stress of members in steel-frame modules

Since the columns, beams and bracings of the MiC modules were modelled as frame elements, the frame component S11 provides the axial stress carried by the module members, with compressive stresses taken as negative. To investigate the long-term stress variations in the module members, the stress distributions of module members at different stages are shown in Figure 13 in terms of the thickness of bar in the respective colour.

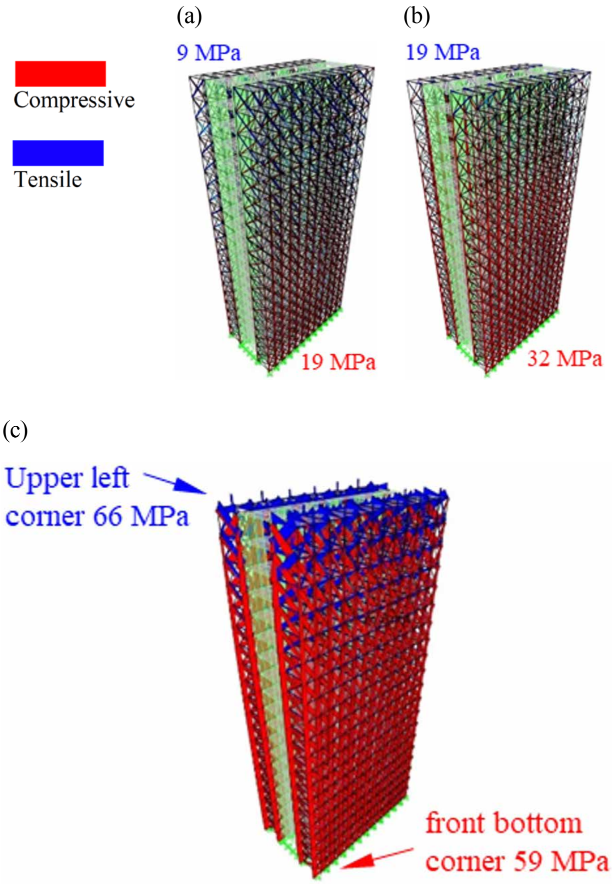

Figure 13. Axial stresses in module members: (a) ignoring time-dependent behaviour; (b) Year 1; and (c) Year 30.

In general, the axial compressive stresses carried by the module columns and the axial tensile stress induced in the module bracings increase over time. Particularly when ignoring concrete time-dependent behaviour, a maximum tensile stress of 9 MPa is observed in the bracing members of modules at the top building corners and a maximum compressive stress of 19 MPa is found in the columns of modules at the bottom storey, which are relatively low compared to the strength of Grade S355 steel. When considering the time-dependent behaviour, the stresses at Year 1 have not changed much, but those at Year 30 have changed significantly. The stresses of two typical modules at Year 30 are shown in Figure 14, including the one at the upper left corner and another at the front bottom corner of the building as shown in Figure 13(c).

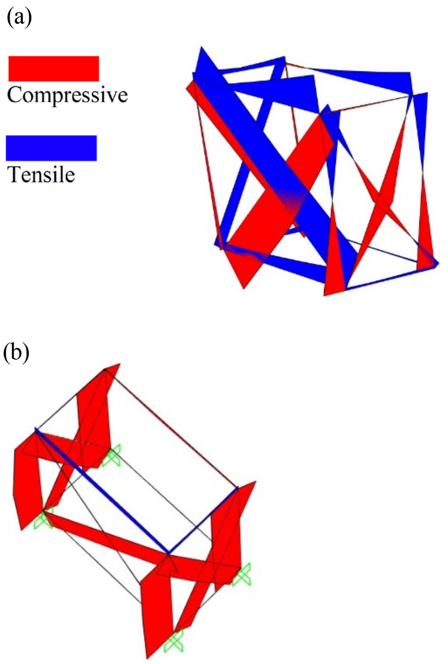

Figure 14. Axial stresses of selected modules of building at Year 30: (a) upper left corner; and (b) front bottom corner.

Figure 14(b) shows that all the column and bracing members in the bottom module are under high compression after 30 years, with the highest compressive stress of 56 MPa observed in one of the columns. Unlike this typical bottom module in compression, the one at the upper left corner is apparently under rather asymmetric loading. Figure 14(a) shows the maximum tensile and compressive stresses in various bracing members as 66 MPa and 59 MPa respectively, indicating a noticeable horizontal force causing distortion of the module, which is consistent with the exaggerated deformation illustrated in Figure 11(a). Although the large stresses observed at Year 30 are still relatively low for Grade S355 steel, they cannot be ignored. In particular, the modules at one side of the bottom storey have to endure huge compressive forces under lateral wind or seismic loading conditions as well. The effects of the long-term behaviour of concrete on the module columns in hybrid MiC building should not be ignored as they tend to reduce the amount of material strength available to resist other loads.

4.4. Long-term axial stress of connections

Two types of connections were used in the hybrid MiC model. Firstly, for the pinned connections between adjacent modules in the same storey, the axial stresses are either in pure compression or pure tension and the axial stress is kept within a low value of 18 MPa when ignoring concrete time-dependent behaviour. There is no evident trend in the distribution of tensile and compressive axial stresses in the same storey. However, when concrete creep and shrinkage are considered, the outer layer of pinned connections are all in tension at Year 1, while the module-to-module connections near the core walls are all in a state of compression, although the maximum axial stress is still around 15 MPa. After 30 years, this roughly uniform stress distribution is still maintained and the maximum compressive stress between modules on Storey 18 near the centre of core walls is 91 MPa, which is consistent with the tensile stresses observed in Figure 12(f).

Secondly, for the module-to-core double-bolt connections, the long-term axial stress of the two anchor rods in each set of module-to-core connections can be quite different under the combined action of shear and tension on the connections. Understandably, the module-to-core connections of the four corner modules carry the heaviest loads as compared with those of the intermediate modules. Among the anchor rods in the corner modules, the anchor rods adjacent to the extreme corners of core walls are under extremely high stresses, while the stresses in the other anchor rods are slightly lower but still larger than those in the other intermediate modules, which is consistent with the observations summarised at the end of Section 4.1. The long-term variations of axial stresses of anchor rods over time are listed in Table 3. Apparently, except for the anchor rods adjacent to the extreme corners of core walls (Figure 6), which will experience significant increases in stress, the concrete creep and shrinkage will induce compressive stresses in some anchor rods of around 187 MPa after 30 years, probably decreasing the safety margin of the Grade 690 anchor rods. In particular, as the anchor rods adjacent to the extreme corners of core walls will be under extremely high stresses (up to 65% of the yield stress) due to concrete creep and shrinkage, the design should be further examined. The solution may be in the form of regular maintenance and adjustment, or provision of strengthened connections at critical locations.

Table 3. Axial stresses in module-to-core double-rod connections at the top storey.

Age	Anchor rods at corners of core walls	Anchor rods elsewhere (range)	
		Tensile	Compressive
Year 1	89 / -85	13 ± 2	-18 ± 8
Year 3	215 / -200	29 ± 2	-58 ± 15
Year 10	331 / -370	49 ± 5	-112 ± 30
Year 20	401 / -452	60 ± 5	-139 ± 35
Year 30	440 / -495	66 ± 6	-151 ± 40
Notes: Tensile stresses are taken as positive; unit: MPa			

4.5. Properties of concrete produced using granitic aggregates

The shrinkage strains of concrete produced using granitic aggregates are known to be higher than those predicted by the British Standards or Eurocodes (British Standards Institution, 2005; Kwan et al., 2010). Therefore, a multiplicative factor has been applied for estimation of shrinkage strains based on the formulae from overseas standards. The ultimate shrinkage strain estimated based on the Code of Practice for Structural Use of Concrete 2013 (Buildings Department, 2013) for the case study is 453×10-6, which is substantially higher than the 296×10-6 estimated according to CEB-FIP Model Code 2010 (fib, 2010) adopted in the analyses. The multiplicative factor in SAP2000 models is kept as 1.0 by default. Obviously, the additional stresses induced would be higher given a larger multiplicative factor for shrinkage strains. To predict such effects more accurately in future studies, it is desirable to obtain more data about the long-term properties of concrete produced locally using granitic aggregates.

5. Conclusions

This paper describes a study of the long-term performance of a typical 20-storey hybrid MiC building considering the creep and shrinkage behaviour of the RC core walls. The hybrid MiC building was modelled by SAP2000 considering the time-dependent behaviour of concrete creep and shrinkage. Based on the numerical results of typical members of the MiC model at different times after construction, the following conclusions can be drawn.

(a) The built-in feature for time-dependent material behaviour and the stepped construction function available in the package SAP2000 provide a convenient tool for investigating the long-term performance of hybrid MiC buildings considering the concrete creep and shrinkage. The modelling techniques described in this paper can be applied to similar projects involving MiC buildings.

(b) The vertical shortening of the core walls of a typical 20-storey hybrid MiC building due to concrete creep and shrinkage is estimated to be 16.0 mm 30 years after commencement of construction. Moreover, the size reduction of the cross section of core walls also tends to distort the modules connected to it. As the concrete creep and shrinkage will induce additional stresses especially in various connections, their safety margin may be adversely affected. It is necessary examine the possible adverse effects due to the time-dependent behaviour of concrete at the design stage so that suitable measures can be taken.

(c) The number of storeys in the MiC building and hence its overall height are key factors as they will govern the shortening of the core walls, as differential axial shortening of various vertical members will induce additional stresses at various components of the building, especially at the connections. When the cross-section dimension of the RC core walls is substantial, the relative horizontal size reduction of the cross section due to concrete creep and shrinkage will also cause additional stresses to be induced at various components of the building, especially at the connections.

(d) It is suggested that checking of long-term performance should be conducted at the design stage for hybrid MiC buildings with RC core walls and steel modules.

However, the present study is based on a typical hybrid MiC building only. While the findings have shed light on the long-term performance of typical multi-storey hybrid MiC buildings, the actual long-term performance of such a building should be estimated by further analyses in view of the numerous factors involved, such as the general arrangement of the building components, structural floor plans, various material properties and construction method.

Acknowledgments

The work described here has been supported by Research Grants Council (Research Impact Fund R7027-18F). The work has also been partially supported by the Ministry of Science and Technology, People's Republic of China (Project No.: 2019YFB1600702).

Notes on contributors

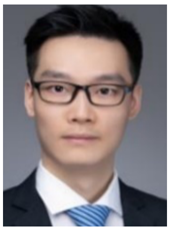

Dr Yingqi Liu is currently an Assistant Professor in the School of Transportation and Logistics at Wuhan University of Technology (WUT), Wuhan. He obtained the degree of Bachelor of Engineering from WUT in 2014. Then he carried out research work in tunnel engineering and graduated with the degree of Master of Engineering from WUT in 2017. He received his Ph.D. degree at The University of Hong Kong (HKU) in 2021, where he had worked on a special earthquake-resistant design of post-tensioned concrete bridge piers. He won an Outstanding Teaching Assistant Award during his study in HKU. His current research interests include rigid body dynamics, seismic isolation and reduction for precast segmental bridges, structural design for MiC buildings, and construction techniques for prefabricated structures.

Mr Ho Kit Siu received his Bachelor's Degree in Civil Engineering with First Class Honours in 2019 from HKU. He is currently an Assistant Engineer at the Water Supplies Department of the Government of the HKSAR. He studied part-time for his Master's Degree in Structural Engineering with his dissertation focusing on the long-term performance of hybrid MiC buildings considering concrete creep and shrinkage.

Mr Shiyu Guan received his Bachelor's degree in Road, Bridge and River covering Engineering from Wuhan University of Technology in 2014. He later worked in projects of China Construction Third Engineering Bureau Group Co., Ltd. and served as Technician, Project Technical Director, Project Chief Engineer and Commercial Director. After registration as a National First-Class Construction Engineer, he was promoted to the Technology and Information Department of the company and currently he is the Vice-Chief Engineer there. He has participated in a key R&D project of Hubei Province and holds some patents. His R&D activities cover BIM and construction methods for prefabricated structures.

Ir Prof Francis T K Au is currently Honorary Professor, and was formerly Professor and Head of the Department of Civil Engineering at HKU. He joined Maunsell Consultants Asia as an engineer upon graduation with his first degree, where he was involved in new town projects, highway projects as well as marine engineering projects. He returned to HKU in 1988 after having seven years of practical experience in the industry. He is engaged in research in bridge engineering and concrete structures. He has also been involved in various engineering projects, including the investigation of Hunghom Station Extension of Shatin-Central Link, investigation of ruptured tendons in Shenzhen Bay Bridge, etc. He has won a number of teaching and research awards, including the R&D Grand Award of Structural Excellence Award 2018 of the Structural Division of the Hong Kong Institution of Engineers.

References

[1] Au FTK and Si XT (2011). Accurate time-dependent analysis of concrete bridges considering concrete creep, concrete shrinkage and cable relaxation. *Engineering Structures*, 33(1), pp. 118-126.

[2] Bažant ZP and Jirásek M (2018). *Creep and hygrothermal effects in concrete structures*. Dordrecht: Springer.

[3] Blanc CM, Sánchez AO and Navarro IF (2021). Analytical characterisation of axial shortening due to creep of reinforced concrete columns in tall buildings. *Engineering Structures*, 228, 111584.

[4] BSI knowledge (2005). *BS EN 1992-2:2005, Eurocode 2. Design of concrete structures – concrete bridges. Design and detailing rules*. London: British Standards Institution.

[5] Buildings Department (2011). *Code of Practice for Dead and Imposed Loads* 2011. Hong Kong: The HKSAR Government.

[6] Buildings Department (2013). *Code of Practice for Structural Use of Concrete* 2013. Hong Kong: The HKSAR Government.

[7] Fédération Internationale Du Béton (fib) (2010). *CEB/FIP Model Code* 2010. Lausanne: International Federation for Structural Concrete. [online]. Available at: < https://www.fib-international.org/publications/model-codes.html>.

[8] Construction Industry Council (CIC) (no date). *MiC projects: overseas significant projects*. [online]. Available at: < https://mic.cic.hk/en/OverseasProjects>.

[9] Construction Industry Council (CIC) (no date). *MiC projects: projects in Hong Kong*. [online]. Available at: <http://mic.cic.hk/en/ProjectsInHongKong>.

[10] Computers and Structures Inc. (no date). *SAP2000 structural analysis and design*. [online]. Available at: < https://www.csiamerica.com/products/sap2000>.

[11] WSP Co. Ltd. (2022). *InnoCell Wins HKIE Structural Excellence Award 2022*. [online]. Available at: <http://www.wsp.com/en-my/news/2022/hkstp-innocell-wins-hkie-structural-excellence-award-2022 >.

[12] Hong Kong Observatory (no date). *Climate of Hong Kong*. [online]. Available at: < https://www.hko.gov.hk/en/cis/climahk.htm>.

[13] Kwan AKH, Au FTK, Wong HHC and Ng PL (2010). Shrinkage of Hong Kong granite aggregate concrete. *Magazine of Concrete Research*, 62(2), pp. 115-126.

[14] Moragaspitiya P, Thambiratnam D, Perera N and Chan T (2010). A Numerical method to quantify differential axial shortening in concrete buildings. *Engineering Structures*, 32(8), pp. 2310-2317.

[15] Pan W and Hon CK (2018). Modular integrated construction for high-rise buildings. *Proceedings of the Institution of Civil Engineers – Municipal Engineer*, 173(2), pp. 1-12.
[16] Shan S and Pan W (2020). Structural design of high-rise buildings using steel-framed modules: a case study in Hong Kong. *The Structural Design of Tall and Special Buildings*, 29(15), pp. e1788.
[17] Shan S, Looi D, Cai Y, Ma P, Chen MT, Su R, Young B and Pan W (2019). Engineering modular integrated construction for high-rise building: a case study in Hong Kong. *Proceedings of the Institution of Civil Engineers – Civil Engineering*, 172(6), pp. 51-57.
[18] Wang Z and Pan W (2020). A Hybrid coupled wall system with replaceable steel coupling beams for high-rise modular buildings. *Journal of Building Engineering*, 31.
[19] Wang Z, Pan W and Zhang Z (2020). High-rise modular buildings with innovative precast concrete shear walls as a lateral force resisting system. *Structures*, 26, pp. 39-53.
[20] Zou D, Du C, Liu T, Teng J and Cheng H (2019). Time-dependent deformations of concrete columns under different construction load histories. *Advances in Structural Engineering*, 22(8), pp. 1845-1854.
[21] Zou D, Liu T, Teng J, Du C and Li B (2014). Influence of creep and drying shrinkage of reinforced concrete shear walls on the axial shortening of high-rise buildings. *Construction and Building Materials*, 55, pp. 46-56.